2021 18th International Conference on Electrical Engineering, Computing Science and Automatic Control (CCE).
Mexico City, Mexico. November 10-12, 2021

Single-Board Computer based Architecture and Firmware for Radiometers with Radio Astronomy applications

Jetzael Cuazoson
IRyA-UNAM
Morelia, Mexico
iee.jetzaelcg@gmail.com

Daniel Ferrusca
Astrophysics Department
INAOE
Puebla, Mexico
dferrus@inaoep.mx

Jesús Contreras
Large Millimeter Telescope
INAOE
Puebla, Mexico
jesuscr.gtm@gmail.com

Eduardo Ibarra-Medel
IRyA-UNAM
Morelia, Mexico
eduardoibarra.medel@gmail.com

Miguel Velázquez
Astrophysics Department
INAOE
Puebla, Mexico
miyang@inaoep.mx

Stan Kurtz
IRyA-UNAM
Morelia, Mexico
s.kurtz@irya.unam.mx

David Hiriart
IA-UNAM
Ensenada, Mexico
hiriart@astro.unam.mx

***Abstract*—We present the electronic architecture of the main control stage and a description of the peripherals' management firmware of a dual-channel water vapor radiometer. The system is based on the *Raspberry Pi* computer with low-cost peripherals to perform data acquisition at 23 and 31 GHz, with capabilities of wireless communication and control mode for remote operation. The system is mounted in the WVR III+ radiometer of the *Hartebeesthoek* Radio Astronomy Observatory of South Africa and its intended use is for sky characterization of existing and future radio astronomical sites.**

***Index Terms*—radiometer, single-board computer, serial communication, wireless, instrumentation**

I. Introduction

Radiometers are instruments to measure noise power from a radiation source. The basic radiometer consists of a radio frequency receiver (mostly heterodyne type) but the complete instrument incorporates multiple devices including sensors, actuators and data recorders [1]. In the astronomical context, water vapor radiometers measure the sky opacity at radio frequencies [2].

In this work, we discuss three different radiometers in order to analyze their structure, deficiencies and capabilities, and to lay the groundwork of our system design from these architectures, looking for autonomy, low-cost, and intuitive use. All three instruments require an external computer either for instrument control or data processing. To improve autonomy and high performance data processing, we present a scalable architecture for control and processing of this type of instrument. Our system is based on the Raspberry Pi [3] single-board computer (SBC) as main control unit. This computer controls data acquisition, servomechanisms, receiver temperature monitoring, and meteorological sensors. It also performs data recording, reduction and uploading to a web server. Due to the versatility of the SBC, the radiometer can be accessed remotely for monitoring and task control.

Funding by CONACYT-NRF grant #291778 and UNAM's DGAPA grant #IT100318.

II. Radiometers

A radiometer is essentially a radio frequency (RF) receiver with various peripherals to perform atmospheric surveys [4]. Fig. 1 shows the basic radiometer structure. It is comprised of an antenna, followed by a filter, typically a Band Pass Filter (BPF), whose technology depends on signal wavelength. The third device is a Square Law Detector (SLD) which is essentially a diode that produces an DC voltage output proportional to the square of the noise voltage of the incoming signal. Finally, an integrator accumulates the input signal over a time interval to produce a representative output which is then recorded.

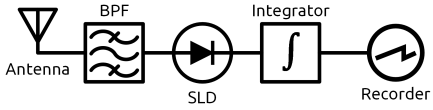

Fig. 1. Basic radiometer block diagram. Details of the design vary with the intended use case [1].

Due to the high frequencies treated in radio astronomy, the RF receivers use the *heterodyne* technique [5] to translate the input frequencies to a lower range, more amenable to the following stages. Radiometers have different electronic architectures that depend partly on the communication interfaces between the receiver and the peripherals. Some radiometers host temperature controllers inside the chassis, dedicated servomechanisms to control the mirrors, weather stations and advanced signal processing stages.

978-1-6654-0029-9/21/$31.00 ©2021 IEEE

A. Survey 3

The *S*urvey 3 is the radiometer of *San Pedro Mártir* Observatory in Baja California, Mexico [6]. The architecture of Survey 3 is based on a microcontroller (MCU) (see Fig. 2) that manipulates the data acquisition and stepper motor control. All the electronics is integrated in a very small space within the radiometer chassis.

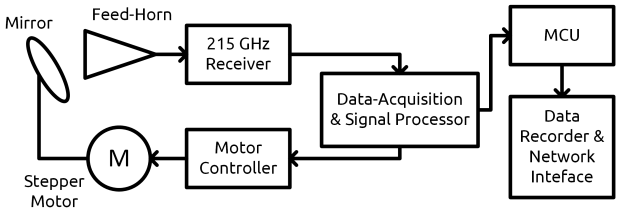

Fig. 2. Survey 3 architecture.

The compactness and versatility of the SBC of the Survey 3 radiometer are desirable features that will serve as a basis for our system. We also take into consideration the simplicity of programming for its sky-tipping routine.

B. RPG-Tip-225

The *R*PG-Tip-225 is the radiometer of the Large Millimeter Telescope in Mexico [7]. The core of this radiometer is an Industrial Personal Computer (IPC) running the Windows® operating system, which performs all the tasks of the radiometer, including the data reduction. The structure of this radiometer is shown in Fig. 3. The IPC runs software that monitors the weather station and the Global Positioning System (GPS). The computer also controls the elevation servomechanism and the heater. The IPC also runs a script to calculate opacity from the measured sky brightness temperature.

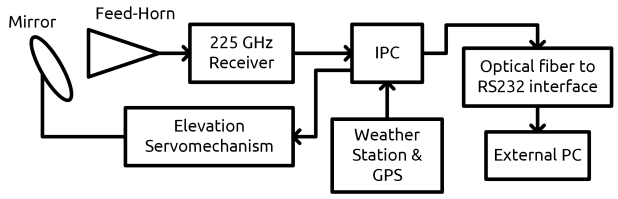

Fig. 3. RPG-Tip-225 architecture.

The RPG-Tip-225 is in operation at the observatory site for sky characterization throughout the year [8]. The opacity data can be accessed remotely to inform observers of the sky conditions. The radiometer also monitors the weather conditions relevant for maintenance tasks on the telescope. The data structure, remote communication modes, connectivity and software processing performance of this radiometer were considered as in developing the design of our system.

C. WVR III

The *WVR III* was formerly the radiometer of the *Hartebeesthoek* Radio Astronomy Observatory (HartRAO) in South Africa. The WVR III has a complex architecture due to its numerous peripherals (see Fig. 4) [9]. The core of the radiometer is based in a personal computer (CPU) which communicates simultaneously with all peripherals through an RS485 to RS232 interface. The MCU controls the observations and data acquisition of the receivers. Both receivers' outputs are DC-signals with three representatives different inputs: antenna, noise source and reference load.

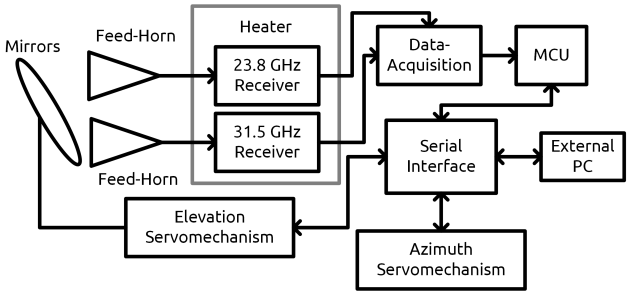

Fig. 4. WVR III architecture.

The WVR III was removed from service in 2007 due to internal failures in the power supply that caused damage to some of the electronics modules, and due to broken cables and non-functioning communication channels [10]. Fortunately, the RF receivers were still operative and it was decided to refurbish the instrument with a new generation architecture to extend its useful life. The refurbishment replaces the data-acquisition, MCU, Serial Interface, External PC stages (hardware components) and optimizes the servomechanism control routines, data structure/processing, sky-survey automation and data sharing (software components).

III. Design of the System

Based on the architectures mentioned above, our team designed an embedded system as an upgrade to the WVR III. In this way, the WVR III+ is introduced. This version has several features that provide autonomy and high-performance to the instrument with a low-cost embedded system based on a SBC [10]. In this section we describe the three main components of WVR III+: the *architecture*, which is the hardware integrated by different electronic devices; the *firmware*, which allows the SBC to communicate with each device; and the *survey code*, which is the software interface to perform sky surveys with the radiometer.

A. Architecture

The embedded system is based on a centralized architecture with multi-protocol interfaces for peripherals (see Fig 5). The WVR III+ consists of nine stages that perform various tasks during the sky surveys:

- **Central processing unit**. Control and monitoring variables of all radiometer subsystems.
- **RF receivers**. Original WVR III receivers (23 & 31 GHz).
- **Scenarios controller**. Control for input signals, antenna, noise source and reference load.
- **Temperature monitor**. Monitoring temperature inside the RF receivers.

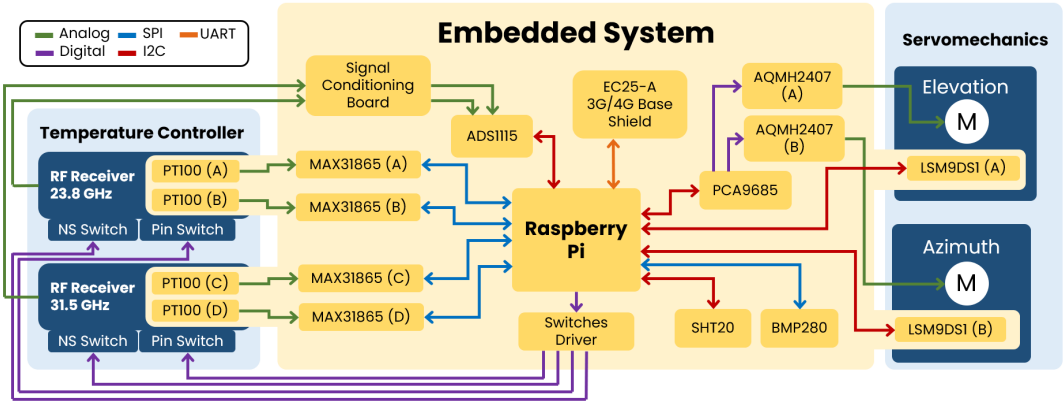

Fig. 5. WVR III+ architecture. The temperature controller is an independent commercial unit that allows different types of control as well as direct self-integrated RTD readout.

- **Signal acquisition**. Conditioning stage for RF signals.
- **Elevation controller**. Control for the elevation angle of mirrors.
- **Azimuth controller**. Control for the radiometer's azimuth motion.
- **Weather station**. Monitoring atmospheric pressure, ambient temperature and humidity.
- **Networks**. 4G network and Ethernet interface.

The system core is the Raspberry Pi 3 B+ (RaspPi). This computer has a General Purpose Input-Output (GPIO) interface that connects to devices using parallel or serial protocols. The peripherals of the system are development boards (dev-boards) made by Adafruit® and all of them can be controlled by Python scripts. The compatibility of the dev-board firmware with the RaspPi environment allows for easy modification of the system parameters according to user needs.

As can be seen, the RaspPi uses many modes of communication with the sub-systems. The system uses analog lines to output the RF signals and all voltages of PT100 sensors. There are six digital 1-bit control lines: four of them control the switching mode inside RF receivers; the remaining two change the orientation of servomechanisms using the DC-DC converters (H-Bridge based). The system uses serial communication protocols such as SPI, UART and I^2C. Table I summarizes the components of the embedded system.

TABLE I
STAGES OF WVR III+

Stage	Elements	Type
CPU	Raspberry Pi 3 B+ [3]	SBC
Scenarios controller	Switches Driver Board (custom design)	Relay interface
Temperature monitor	PT100 [11] (A, B, C, D) MAX31865 [11] (A, B, C, D)	RTD RTD digital interface
Signal acquisition	Signal conditioning (custom design) ADS1115 [11]	Op-Amp amplifier ADC
Elevation controller	LSM9DS1 [11] (A) AQMH2407 [12] (A) PCA9685 [11] (CH0)	IMU DC-DC Converter PWM interface
Azimuth controller	LSM9DS1 (B) AQMH2407 (B) PCA9685 (CH1)	IMU DC-DC Converter PWM interface
Weather station	BMP280 [11] HTU21 [11]	Pressure Sensor Ambient Temp. & Humidity sensor
Networks	EC25-A [13] 3G/4G Base shield [13]	4G network adapter EC25 board interface

B. Firmware

Each component of the system was tested individually to understand its operation mode using python codes executed from the RaspPi. Every board was programmed as an object to provide attributes that can be easily used in the *Survey code*. These codes are integrated into a single script that sequentially executes each code. This script is known as the **hardware module**; its flow chart is shown in Fig. 6 and we describe its functions below.

- **Temperature monitor script**. This code requests data from each MAX31865 board and implements a median-filter to pre-process the data. The temperatures are then recorded into the RaspPi.
- **Servomechanism control script**. This program tests two different discrete-time controllers. The first one is a *PI* controller for elevation angle and the second is a *P* controller for azimuth angle. Both are based on similar control chains but using separate devices. Both azimuth and elevation IMUs have different operation modes and accuracies for survey purposes. Each controller reads the angle input using a single LSM9DS1 IMU; this angle is then compared to the setpoint angle. After that, the RaspPi executes the control law and sends a representative pulse-width value to the respective channel of the PCA9685. This board enables a Pulse-Width Modulation (PWM) signal while the RaspPi enables the servos orientation using the AQMH2407 power stages. Finally, the servomechanisms are set and the angle is fed back to the RaspPi. The control loops are executed separately and sequentially, so the PWM signals of each servomecha-

nism are sent in their respective loops. Since the features of elevation and azimuth DC-motors, and their plants, are different both electrically and mechanically, we used two different power stages, each with the appropriate capabilities, to interact with these motors.

- **RF signal acquisition script**. The conditioned DC-signals from the SLDs of the RF receivers (both 23 & 31 GHz channels) are acquired and digitized by the ADS1115. After that, the RaspPi implements a gain compensation to recover the input signal. Since the radiometer uses the *Dicke* technique [14], the signal is acquired while radiometer cycles through the three scenarios mentioned in Sec. II-C.
- **Weather monitor script**. In the same way as the temperature monitor code, this script requests ambient temperature and relative humidity data from the HTU21 board and barometric pressure data from the BMP280 board. These data are then recorded by the RaspPi.
- **Data logger script**. This code has two different purposes: it collects all the acquired data into a text file that is stored both internally in the RaspPi and on the web server, and it also helps the *Survey code* detect execution errors during the survey. All data time series breaks are recorded into a text file to provide a operations log for the user.

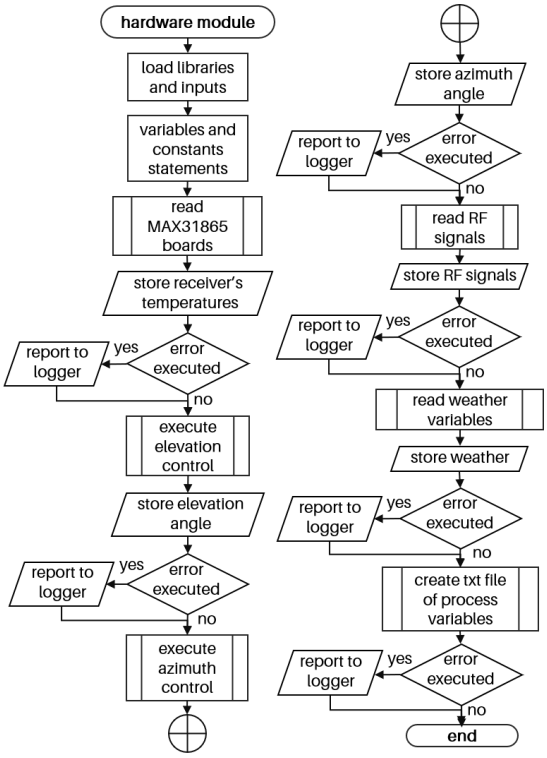

Fig. 6. WVR III+ firmware flow chart.

C. Survey Code

This script is the main program of the system; it is called **wvrsa** in the RaspPi. This code performs a sky survey with the WVR III+ using the new core and firmware to communicate with each sub-system for request and control data.

The script is based on the operation mode used by the *Survey 3* radiometer. First, the desired elevation/azimuth angles are set along with the switches specifying the receiver's input sequence. Then the observing cycle time is set at the user's discretion. In the following processes, the attributes of **hardware module** are used to do system checking. Hardware checking is executed to ensure that there are no undesirable angles or nonsensical temperatures of the receivers. The voltages of the RF stages are checked to confirm reasonable values. Next, a sub-process determines the number of repetitions of the survey process using the specified observing cycle time. Finally, the survey process is executed by setting up the servomechanisms, reading the receiver temperatures, acquiring the RF signals and reading the weather variables. If an error occurs during the survey, **wvrsa** stops execution immediately. The flow of the above processes is subject to user decisions through a keyboard interrupt or *SystemExit* module (OS native module). There is also a section for reporting of unexpected errors. The flow chart of **wvrsa** is shown in Fig. 7.

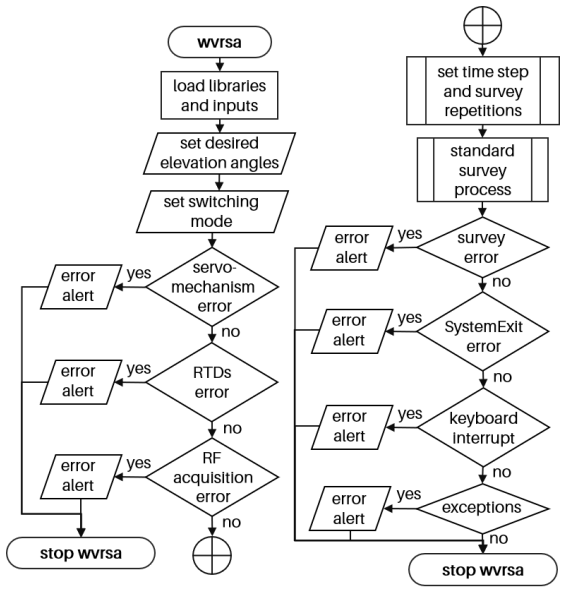

Fig. 7. Survey code flow chart of WVR III+.

In addition to the survey code, an independent script is executed to upload the report file to the GDrive® cloud server. For this task, the system uses a *daemon* [15] to schedule the execution of various scripts at a certain time. For our purposes, the system activates the 4G network via the UART bus and waits for internet connection availability. Once this is approved, the system looks for the report file and uses Google® services to access the server. After that, the file is uploaded and the system sends a notification to the user via email or Short Message Service (SMS). Finally, the 4G interface is turned off to avoid electromagnetic interference (EMI) for the following sky sweep.

The radiometer was subjected to various tests following the original survey methodology of WVR III to confirm proper operation of the included software based on LabVIEW®. This software computes precipitable water vapor (PWV) and

path delay from the detected RF power levels according to user configurations. Taking this into consideration, the RaspPi generates a report file with the same structure as used by WVR III. This file is stored in the host computer.

IV. Results

The developed system has shown autonomy and enhanced performance to operate atmospheric sky surveys and consequently calculate PWV and opacity. Below we describe the main results obtained that validate the capabilities of the WVR III+ with the new embedded system [10].

The switching speed of RaspPi's GPIO and the response of the *scenarios controller* board allows the switching of the signal periods to have similar times as with the original boards, with a period of 15.3 seconds. The logical high (active-high) times was 3.9 seconds for the switch of the noise source, 7.95 seconds for the antenna switch (active-low) and 3.45 seconds for reference load (active high) in both channels.

The Bode-analysis of the *signal acquisition* board shows that the allowed bandwidth guarantees linear amplification up to $f \leq 10^4$ Hz (see Fig. 8). This bandwidth eases the digitization and software compensation of the three DC-signal sources of the radiometer. Before signal conditioning, the SLD outputs of the RF receivers are constant voltages when noise source and reference load are connected and very low frequency signals ($f < 1$ Hz) when the antenna is connected.

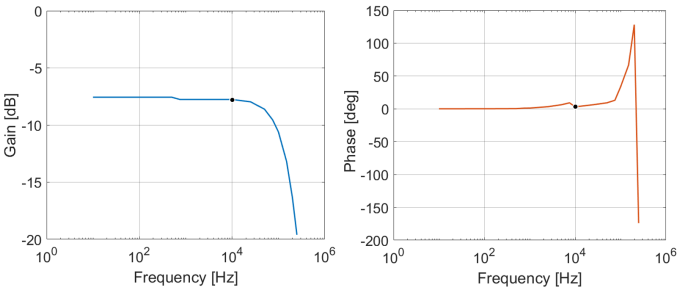

Fig. 8. Bode plots for *signal acquisition* board. Linear gain and in-phase signals are seen for frequencies less than 10 kHz.

The elevation and azimuth plants and controllers were characterized using MATLAB® toolboxes. After discrete-time implementation into RaspPi, the control system guarantees an accuracy of 0.5 degrees via software for elevation angle and 1.0 degree for azimuth angle, with an discretization time of $\sim 8 \pm 0.2$ milli-seconds per iteration of control script. Both scripts use an internal clock of the RaspPi to ensure a uniform discretization time. Several tests were performed with angles similar to those used in field, such as: 89.8, 40.1, 29.9, 19.2 and 14.4 elevation degrees with fixed azimuth angle. Each elevation angle is called an *air mass* [16] while the set of angles is called the *observed sky*. The air mass routine takes around 1 minute and the observed sky routine time depends on the air mass sequence defined by the user. The time response (during characterization) of each system is shown in Fig. 9. Since the azimuth mechanism does not need to be as accurate as elevation, a proportional controller satisfied the needs of this mechanism. To ensure proper positioning, each control loop waits for at least 3 seconds in steady state after reaching the setpoint.

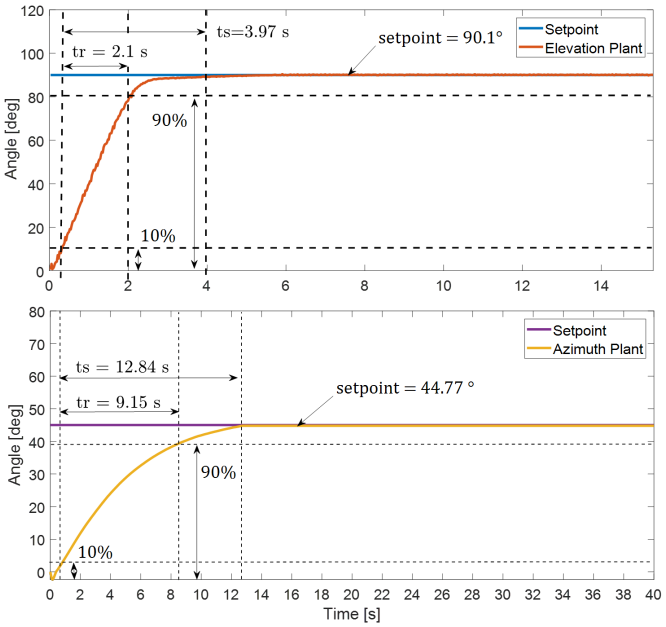

Fig. 9. Servomechanism time response using controllers.

The ambient temperature monitoring system was relative easy to implement by using the Adafruit® dev-boards and its virtual interface. However, we implemented a custom median filter in order to avoid abrupt changes in small periods of time due to communication loss with the MAX31865 boards. The input parameters of the median filter (custom design) allow a reading accuracy of 0.2 degrees.

The meteorological parameters given by the HTU21 board are acquired with a sampling period of 8 seconds while the BMP280 has a sampling period of ~ 0.5 seconds, according to manufacturer's specifications. The sensors are not in continual operation because the acquisition of meteorological data is done at the user's request; in this case, the data is requested every *observed sky* cycle and repeated during the *air mass* routine. These acquisition times are adequate for our purposes because the weather data vary slowly, compared to other system variables.

The code *hardware module* collects data from each stage of the system. The data values are requested on-demand and stored as a text file in the RaspPi registers. The text file is arranged into 17 columns as follows:

- Date-Time. Single column. String type variable.
- Setpoint angles. One column for azimuth, one column for elevation. Float type variables.
- Driven angles. One column for azimuth, one column for elevation. Float type variables.
- PT100 temperatures. Four columns for 4 PT100 sensors. Float type variables.
- Receiver voltages. Six columns: antenna, noise source and reference load for two (23 & 31 GHz) receivers.

Float type variables.

- Weather parameters. One column for outdoor temperature, one column for barometric pressure. Float type variables.

The radiometer was tested with Ethernet and WiFi networks as well as 4G using local cell phone services, which validate the use of the EC25-A and 3G/4G base boards.

The *Survey code* provides a completely customizable environment with a well-defined data structure that allows an intuitive manipulation of the instrument from the software.

It is important to mention that radiometers are manufactured in a custom way according to user's needs. Hence, the features differ between instruments and it is difficult to compare them in a general way. On the other hand, the commercial demand of radiometers is sufficiently low that the manufacture of these instruments is mostly managed by specific groups at research institutes and universities. Hence, the technical documentation regarding radiometers in radio astronomy observatories is rather limited. We present in Table II the primary specifications that were obtained from the experiments. These parameters relevant for the technical treatment of the instrument by HartRAO users.

TABLE II
MAIN TECHNICAL DETAILS OF WVR III+

Feature	**Value**			**Units**
	min	***nom***	***max***	
Time delay of switching signals	20	24	–	μs
Signal conditioner bandwidth	10^{-3}	–	10^{3}	Hz
Elevation accuracy	–	± 0.5	–	deg
Azimuth accuracy	–	± 1.0	–	deg
Temperature accuracy	–	± 0.2	–	°C
Weather station sample time	9	12	15	s
Air mass cycle time	0.8	1	1.25	min
Radiometer's Allan time	–	15	–	s

V. CONCLUSIONS

We have successfully upgraded the WVR III to a new version, WVR III+, which not only fulfills the original demands of the radiometer but also provides new capabilities such as wireless communication via WiFi, 4G networks or Ethernet, along with an open source code to control and monitor the system. These tasks are possible thanks to the use of the Raspberry Pi 3 B+, which provides both a graphic and command line operating system, and by the subsystems, which accomplish their respective tasks in the sky-tipping environment within the regime of stable meteorological conditions.

Firmware and Survey codes were tailored to provide an intuitive object-oriented code that can be easily modified if particular needs are required for certain types of sky observations. Once the WVR III+ is returned to operation at HartRAO, it will be tested to evaluate its performance and reduction method. We also plan side-by-side tests of the Survey 3 and RPG-Tip-225 during the coming year in order to correlate atmospheric opacity at their respective frequency bands and evaluate sky characterization methods within those bands [17].

ACKNOWLEDGMENTS

We are grateful to the *CONACYT-NRF* bilateral program South Africa-Mexico for funding the project **291778** "*Development of technology, data and capacity in millimeter water vapor radiometry for radio astronomy*". We also thank UNAM's *DGAPA* for funding the project **IT100318** "*Advanced technologies for water vapor radiometry*".

We especially thank the staff of HartRAO for providing the WVR III and entrusting us with its refurbishment. This work would not have been possible without the assistance of Prof. Tinus Stander of the University of Pretoria, who gave us essential technical and theoretical support regarding the instrument as well as shipping paperwork and custom matters.

REFERENCES

[1] N. Skou, D. M. Le Vine, "Microwave Radiometer Systems: Design and Analysis," 2nd Ed., Artech House, 2006. ISBN-13 9781580539746,

[2] F. D. Drake and H. I. Ewen, "A Broad-Band Microwave Source Comparison Radiometer for Advanced Research in Radio Astronomy," Proc. IRE, Vol. 46, No. 1, 1958. doi: 10.1109/JRPROC.1958.286710

[3] R. P. Foundation. "Raspberry Pi 3 Model B+ Documentation," Raspberry Pi Foundation, 2021. Available: https://www.raspberrypi.org/

[4] T. L. Wilson, K. Rohlfs, S. Hüttemeister, "Tools of Radio Astronomy," 5th ed., Springer, 2009. doi: 10.1007/978-3-540-85122-6

[5] D. Pozar. "Microwave Engineering," 4th Ed., Wiley, 2011. ISBN 9780470631553

[6] D. Hiriart. "Survey 3 Owner's Manual and Radiometer Utilities," Institute of Astronomy, National Autonomous University of Mexico, 1994.

[7] D. Ferrusca, J. Contreras, "Weather monitor station and 225 GHz radiometer system installed at Sierra Negra: the Large Millimeter Telescope site," Proc. SPIE 9147, Ground-based and Airborne Instrumentation for Astronomy V, 2014. doi: 10.1117/12.2055005

[8] M. Zeballos, D. Ferrusca, J. Contreras, D. H. Hughes. "Reporting the first 3 years of 225-GHz opacity measurements at the site of the Large Millimeter Telescope Alfonso Serrano," Proc. SPIE 9906, Ground-based and Airborne Telescopes VI, 2016. doi: 10.1117/12.2232168

[9] C. GmbH. "WVR III (microwave water-vapor radiometer) technical documentation," ETH Institute of Geodesy and Photogrammetry, 2000.

[10] D. Ferrusca, J. Cuazoson. J. Contreras, D. Hiriart, E. Ibarra, S. Kurtz, T. Stander and M. Velázquez. "Embedded system upgrade based on Raspberry Pi computer for a 23/31 GHz dual-channel water vapor radiometer," Proc. SPIE Vol. 11445: Ground-based and Airborne Telescopes VIII, 1144586, 2020. doi: 10.1117/12.2561733

[11] L. Ada, T. DiCola, K. Rembor, B. Earl, B. Bearnes, C. Nelson and D. Nosonowitz. "Adafruit Explore & Learn Breakout Boards," Adafruit Industries LLC, 2021. Available: https://learn.adafruit.com/

[12] D. Wiki. "7A Dual DC Motor Driver," DFRobot Documentation, 2017. Available: https://wiki.dfrobot.com/

[13] S. Incorporation. "QMI Interface with Sixfab Shields/HATs," SixFab Documentation, 2018. Available: https://sixfab.com/

[14] L. Strom, "The theoretical sensitivity of the Dicke radiometer" WESCON/57 Conference Record, 1957, pp. 188-193, doi: 10.1109/WESCON.1957.1148713

[15] D. Lennert. "How To Write a UNIX Daemon," Hewlett-Packard Company, 2007. Available: http://cjh.polyplex.org/

[16] R. Mathar. "Astronomical Air Mass," Max-Planck Institute of Astronomy. 2015. Available: https://www2.mpia-hd.mpg.de/

[17] T. Stander, R. Deane, D. de Villiers, A. de Witt, D. Ferrusca, D. Hiriart, S. E. Kurtz, F. van den Heever, M. Velázquez. "Progress toward improved water vapour radiometry: an overview of the South Africa-Mexico bilateral programme," Proc. SPIE 11445, Ground-based and Airborne Telescopes VIII, 2020. doi: 10.1117/12.2562017